Editors' Suggestion

Stochastic Dynamics of Incoherent Branched Flows

Josselin Garnier,[1] Antonio Picozzi,[2] and Theo Torres[2]

[1]*CMAP, CNRS, Ecole polytechnique, Institut Polytechnique de Paris, 91120 Palaiseau, France*

[2]*Université Bourgogne Europe, CNRS, Laboratoire Interdisciplinaire Carnot de Bourgogne,ICB UMR 6303, 21000 Dijon, France*

(Received 12 February 2025; revised 8 April 2025; accepted 30 April 2025; published 3 June 2025)

Waves propagating through weakly disordered smooth linear media undergo a universal phenomenon called branched flow. Branched flow has been observed and studied experimentally in various systems by considering coherent waves. Recent experiments have reported the observation of optical branched flow by using an incoherent light source, thus revealing the key role of coherent phase-sensitive effects in the development of incoherent branched flow. By considering the paraxial wave equation as a generic representative model, we elaborate a stochastic theory of both coherent and incoherent branched flow. We derive closed-form equations that determine the evolution of the intensity correlation function, as well as the value and the propagation distance of the maximum of the scintillation index, which characterize the dynamical formation of incoherent branched flow. We report accurate numerical simulations that are found in quantitative agreement with the theory without free parameters. Our theory highlights the important impact of coherence and interference on branched flow, thereby providing a framework for exploring branched flow in nonlinear media, in relation to the formation of freak waves in oceans.

DOI: 10.1103/PhysRevLett.134.223803

Introduction—Waves passing through a weakly disordered smooth medium with a correlation radius larger than the wavelength form long, narrow filaments called branches. Instead of random speckle patterns, the disordered potential focuses waves into branches that split, creating a treelike structure, known as branched flow (BF). Originally observed in electrons [1–5] and microwave cavities [6,7], BFs have been anticipated to occur with vastly different wavelength scales [8]. They may serve as a catalyst for the emergence of extreme nonlinear events [9–13], and freak waves on the ocean [14–19]. BFs have also been suggested to occur for sound waves [20], ultrarelativistic electrons in graphene [21], flexural waves in elastic plates [22], while they can act as a conduit for energy transmission in scattering media [23]. BFs have been extended to random potentials in space and time [24], to periodic potentials [25,26], and even to active random walks [27]. More recently, BFs have been observed experimentally with optical waves propagating in soap films [28], and the control of light BF through weakly disordered media has become an important challenge [23,29–31].

The formation of BFs can be explained using geometrical optics, where local maxima of the random refraction index act as lenses, creating caustics and high wave intensities, as originally described in Refs. [32,33]. Numerical simulations show that the scintillation index (i.e., the relative variance of the intensity fluctuations) can exceed one in such cases. Recent studies have used geometrical optics or diffraction integrals in the framework of catastrophe optics [34,35] to derive the scaling behavior of BF dynamics [36,37] and extreme waves [38,39]. Actually, except for some particular theoretical studies [40,41], BFs have been essentially treated in the framework of ray caustics, then disregarding coherence or interference effects [8]. Along this way, experiments have been carried out essentially with coherent waves, such as coherent electron waves [1], coherent microwaves [6,7], or with coherent laser light [28]. On the other hand, in recent experiments, optical BFs have been studied by using incoherent light sources [42], revealing intriguing properties about the role of coherence in the formation and the evolution of BFs, such as coherent interference between the different wave fronts and the sensitivity of BFs to the coherence of the waves.

Our aim in this Letter is to elaborate a stochastic formulation of BFs by considering an initial random wave function propagating in a random potential. Using the paraxial wave (Schrödinger) equation as a representative model, we show that interference effects deeply modify the statistical properties of BFs. Employing multiscale and stochastic calculus, we derive closed-form equations that give the evolution of the intensity correlation function. In particular we describe the evolution of the scintillation index that characterizes the dynamical formation of incoherent BFs. We determine that the scintillation index is a function of two dimensionless parameters that we identify and that involve the statistics of the medium and of the initial field. The theory of the stochastic dynamics of BFs is validated by accurate numerical simulations, which are found in quantitative agreement with the theory, without using any adjustable parameter.

Model—We consider the two-dimensional paraxial wave equation [43,44]:

$$i\partial_z\psi_z = -\alpha\partial_x^2\psi_z + V(z,x)\psi_z, \quad z>0, x\in\mathbb{R}, \tag{1}$$

starting from $\psi_{z=0}(x) = \psi_o(x)$, where ψ_o is a coherent or partially coherent field and V is a smooth and slowly varying potential, which we assume to be a random process. We will denote by $\mathbb{E}[\cdot]$ the expectation with respect to the distribution of this random process.

We present our work in optics as a concrete example, but the paraxial wave Eq. (1) is widespread in physics, making the processes discussed herein broadly applicable to various systems. In optics, the parameter α and the potential V are related to the index of refraction n as follows: $\alpha = 1/(2k_o n_o)$, $V(z,x) = k_o[n_o^2 - n^2(z,x)]/(2n_o)$, where k_o is the wave number in free space, n_o is the homogeneous background index of refraction, and $n(z,x)$ is the spatially dependent index of refraction of the medium.

We will consider two different types of initial field.

(1) We will first consider the coherent case in which the initial field is a plane wave: $\psi_o(x) = 1$. The measured intensity is $|\psi_z(x)|^2$, the mean intensity is $\mathbb{E}[|\psi_z(x)|^2]$, and the scintillation index (i.e., the relative variance of the intensity) is

$$S_z(x) = \frac{\mathbb{E}[|\psi_z(x)|^4] - \mathbb{E}[|\psi_z(x)|^2]^2}{\mathbb{E}[|\psi_z(x)|^2]^2}. \tag{2}$$

(2) We will then consider, in detail, the situation in which the initial field is a coherent or partially coherent speckled field. We will consider the two following situations:

`(c)` ψ_o is a coherent speckled field, which will be modeled as a stationary random field with Gaussian statistics and correlation radius ρ_o (the width of the field correlation function).

`(pc)` ψ_o is a partially coherent speckled field, which will be modeled as a time-dependent random field with Gaussian statistics and correlation radius ρ_o. Such fields can be generated by passing a time-harmonic plane wave through a static [case `(c)`] or rotating [case `(pc)`] diffuser, which features a random arrangement of scattering centers. This experimental setup has attracted considerable interest due to its ability to mimic the properties of a thermal light source [45,46], with the added advantage of controlling the spatial and temporal coherence properties from the degree of roughness of the diffuser and its rotation speed. It has been used to investigate speckle phenomena [46], ghost imaging [47,48], and incoherent BFs [42].

We will denote by $\langle\cdot\rangle$ the expectation with respect to the distribution of the initial field. In situation `(c)`, the measured intensity is $|\psi_z(x)|^2$, the mean intensity is $\mathbb{E}[\langle|\psi_z(x)|^2\rangle]$, and the scintillation index is

$$S_z^{(c)}(x) = \frac{\mathbb{E}[\langle|\psi_z(x)|^4\rangle] - \mathbb{E}[\langle|\psi_z(x)|^2\rangle]^2}{\mathbb{E}[\langle|\psi_z(x)|^2\rangle]^2}. \tag{3}$$

In situation `(pc)`, assuming that the response time of the photodetector is larger than the coherence time of the field, the measured intensity is $\langle|\psi_z(x)|^2\rangle$ (the averaging $\langle\cdot\rangle$ is experimentally carried out by time averaging by the detector over the multiple initial conditions generated by the rotating diffuser), the mean intensity is $\mathbb{E}[\langle|\psi_z(x)|^2\rangle]$, and the scintillation index is

$$S_z^{(pc)}(x) = \frac{\mathbb{E}[\langle|\psi_z(x)|^2\rangle^2] - \mathbb{E}[\langle|\psi_z(x)|^2\rangle]^2}{\mathbb{E}[\langle|\psi_z(x)|^2\rangle]^2}. \tag{4}$$

Coherent initial plane wave—In this paragraph we assume a regime in which (i) the wavelength $\lambda = 2\pi/k_o$ is much smaller than the correlation radius ℓ_c of the index of refraction of the medium; (ii) the variance σ_n^2 of the index of refraction is small (hence, the variance $\sigma^2 = 4\pi^2\sigma_n^2/\lambda^2$ of the random potential satisfies $\sigma^2 \ll 1/\lambda^2$); (iii) the propagation distance is large enough so that the evolution of the variance of the intensity is of order one.

This situation has been intensively studied [43,49]. By a multiscale analysis, closed-form equations can be derived for the field and intensity correlation functions [50,51]. These equations depend on the medium statistics via the integrated medium correlation function γ defined by

$$\gamma(x) = \int_{\mathbb{R}} \mathbb{E}[V(0,0)V(z,x)]dz, \tag{5}$$

which can be written in the form $\gamma(x) = \sigma^2\ell_c\tilde{\gamma}(x/\ell_c)$. As a particular example of a smooth random medium, we can consider a medium with Gaussian correlation function $\mathbb{E}[V(0,0)V(z,x)] = \sigma^2\exp(-(x^2+z^2)/\ell_c^2)$, so that $\tilde{\gamma}(\tilde{x}) = \sqrt{\pi}\exp(-\tilde{x}^2)$. The field correlation function is $\mathbb{E}[\psi_z(x+(y/2))\bar{\psi}_z(x-(y/2))] = \exp[z(\gamma(y)-\gamma(0))]$ [50]. This shows that the mean intensity is constant in z and x and that the correlation radius of the field decays as $1/\sqrt{z}$ [52].

We introduce two relevant parameters that will play a key role: $X_c = \sigma^{2/3}\ell_c/\alpha^{1/3}$ (which is dimensionless) and $z_c = \ell_c/(2\sigma^{2/3}\alpha^{2/3})$ (which is homogeneous to a length), that will be shown to correspond to the propagation distance at which the scintillation index reaches a maximum for large values of X_c. They can also be expressed as $X_c = (2^{4/3}\pi n_o^{1/3})\sigma_n^{2/3}\ell_c/\lambda$ and $z_c = (2^{-1/3}n_o^{2/3})\ell_c/\sigma_n^{2/3}$. From Ref. [50] we find that the scintillation index does not depend on x:

$$S_z = \tilde{D}_{z/z_c}(0,0) - 1, \tag{6}$$

where $\tilde{D}_{\tilde{z}}(\tilde{x},\tilde{y})$ satisfies

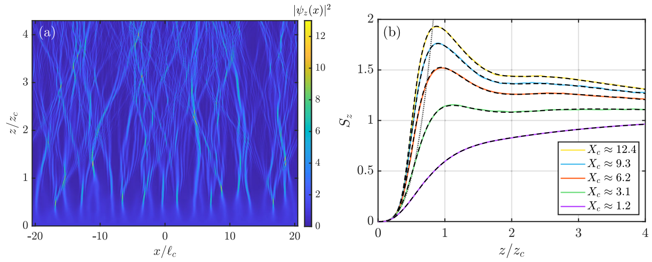

FIG. 1. Coherent initial plane wave with a medium with Gaussian correlation: (a) Numerical simulation of Eq. (1) showing the evolution of $|\psi_z(x)|^2$ starting from $\psi_o(x) = 1$. Parameters: $\ell_c/\lambda = 100$, $\sigma^2\lambda^2 = 10^{-4}$ ($X_c \approx 12.4$). (b) Scintillation index S_z versus z/z_c for different values of X_c: the black dashed lines report the theory, Eq. (6); the dotted line is the small z prediction $S_z \simeq 2\sqrt{\pi}(z/z_c)^3$; the colored lines are the results of the numerical simulations, averaged over 1000 independent realizations of the disordered potential. Parameters: from the bottom, $\ell_c/\lambda = 10$, 25, 50, 75, with $\sigma^2\lambda^2 = 10^{-4}$ for all curves, except for the top yellow curve ($X_c \approx 12.4$) where $\ell_c/\lambda = 50$, $\sigma^2\lambda^2 = 8 \times 10^{-4}$.

$$\partial_{\tilde{z}} \tilde{D}_{\tilde{z}} = iX_c^{-1} \partial_{\tilde{x}} \partial_{\tilde{y}} \tilde{D}_{\tilde{z}} + \frac{1}{2} X_c^2 \tilde{\mathcal{U}}(\tilde{x}, \tilde{y}) \tilde{D}_{\tilde{z}}, \tag{7}$$

starting from $\tilde{D}_{\tilde{z}=0}(\tilde{x}, \tilde{y}) = 1$, with $\tilde{\mathcal{U}}(\tilde{x}, \tilde{y}) = 2\tilde{\gamma}(\tilde{x}) + 2\tilde{\gamma}(\tilde{y}) - \tilde{\gamma}(\tilde{x} + \tilde{y}) - \tilde{\gamma}(\tilde{x} - \tilde{y}) - 2\tilde{\gamma}(0)$ [here $\tilde{x} = x/\ell_c$ and $\tilde{y} = y/\ell_c$]. This shows that the scintillation index is a function of $\tilde{z} = z/z_c$ and X_c only. Equation (7) can be solved by the split-step Fourier method [53]. Moreover, by expanding the solution for small $\tilde{z}$, we get $S_z \simeq [\partial_{\tilde{x}}^4 \tilde{\gamma}(0)/6](z/z_c)^3$ at leading order [with $\partial_{\tilde{x}}^4 \tilde{\gamma}(0) = 12\sqrt{\pi}$ for a medium with Gaussian correlation].

Here are the main results.

First, the scintillation index S_z is close to 0 when z is small (i.e., smaller than z_c) and it first increases cubically with z.

Second, when X_c is below a threshold value $X_c^{(\mathrm{t})}$ [$X_c^{(\mathrm{t})}$ is between one and three for a medium with Gaussian correlation function, see Fig. 1(b)], the scintillation index is monotonically increasing towards its limit value 1 when $z \to +\infty$.

Third, when X_c is above the threshold value $X_c^{(\mathrm{t})}$, the scintillation index reaches a maximal value larger than one at finite propagation distance. The maximal value $\max_z S_z$ depends only on X_c, but the distance z at which the maximum of the scintillation index is reached depends on X_c and z_c (it was predicted to be proportional to $\ell_c/\sigma_n^{2/3}$ in previous works [32,33]). It then relaxes to its limit value 1 when $z \to +\infty$, where the wave field acquires Gaussian statistics for very large propagation distances [38,51,54–56].

Finally, it is quite surprising to note that when X_c is larger than $X_c^{(\mathrm{t})}$, then the scintillation index may present two maxima, one global and one local [see the small bump around $z/z_c = 2.5$ in Fig. 1(b)].

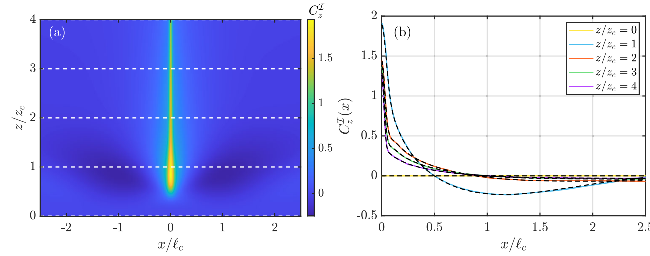

FIG. 2. Coherent initial plane wave with a medium with Gaussian correlation. (a) Theoretical intensity correlation function $C_z^{\mathcal{I}}(x)$ from Eq. (9). (b) Comparison of $C_z^{\mathcal{I}}(x)$ from Eq. (9) (black dashed lines), with the numerical simulations of Eq. (1) (colored lines), for different propagation lengths z/z_c. An average over 1000 simulations with different realizations of the random potential $V(z, x)$ has been carried out. Parameters: $\ell_c/\lambda = 100$, $\sigma^2\lambda^2 = 10^{-4}$ ($X_c \approx 12.4$).

We remark that the distance $\ell_c/\sigma_n^{2/3}$ is also the typical spatial scale of evolution of the number of branches that a Hamiltonian flow develops in a random potential [37]. As discussed in Ref. [57], sec. I, a ray theory of branched flow can predict the numbers and positions of local intensity maxima, however it cannot predict the values of the maxima that result from interference effects and that depend on the coherence properties of the initial field (see also [41]).

We have also computed the intensity correlation function

$$C_z^{\mathcal{I}}(x) = \frac{\mathbb{E}[|\psi_z(y + \frac{x}{2})|^2 |\psi_z(y - \frac{x}{2})|^2] - \mathbb{E}[|\psi_z(y)|^2]^2}{\mathbb{E}[|\psi_z(y)|^2]^2}, \tag{8}$$

which is independent of y and is given by

$$C_z^{\mathcal{I}}(x) = \tilde{D}_{z/z_c}(x/\ell_c, 0) - 1, \tag{9}$$

where $\tilde{D}$ is the solution of Eq. (7). The intensity correlation function is plotted in Fig. 2. Of course one has $C_{z=0}^{\mathcal{I}}(x) = 0$, $C_z^{\mathcal{I}}(0) = S_z$, $C_z^{\mathcal{I}}(x) \to 0$ as $x \to +\infty$, and $\int C_z^{\mathcal{I}}(x) dx = 0$ (this can be interpreted as an energy conservation relation).

We have tested the validity of the theoretical predictions by direct numerical simulations of the paraxial wave Eq. (1) (see Ref. [57], sec. VIII). The results for the evolution of the scintillation index in Fig. 1 and the intensity correlation function in Fig. 2 show excellent quantitative agreements, even though the separation of scales is not strong in the simulations.

Incoherent initial wave: Scaling regime—From now on we address the situation in which the initial field $\psi_o(x)$ is a speckled field. In addition to the assumptions (i) to (iii) considered above for the initial plane-wave case, we assume that $\psi_o(x)$ has Gaussian statistics, with correlation radius ρ_o larger than the wavelength λ and smaller than the correlation radius ℓ_c of the index of refraction, $\ell_c/\lambda \gg \rho_o/\lambda \gg 1$.

We carry out a multiscale analysis in which a small, dimensionless scale parameter ε encapsulates the four assumptions listed above. Accordingly, we denote by $\varepsilon \sim \lambda/\ell_c$, the order of magnitude of the ratio of the wavelength over the correlation radius of the index of refraction. We assume that the typical amplitude of the fluctuations of the index of refraction is ε^c, with $c > 0$. If we consider that the reference length is the correlation radius of the index of refraction, we can write $\alpha^\varepsilon = 1/(2k_o n_o) = \varepsilon\alpha$ and $V^\varepsilon = k_o(n_o^2 - n^2)/(2n_o) = \varepsilon^{c-1}V$, and the scaled paraxial wave equation has the form

$$i\partial_z \psi_z^\varepsilon = -\varepsilon\alpha\partial_x^2\psi_z^\varepsilon + \varepsilon^{c-1}V(z,x)\psi_z^\varepsilon, \quad z>0, x\in\mathbb{R}, \tag{10}$$

starting from $\psi_{z=0}^\varepsilon(x) = \psi_o^\varepsilon(x)$. The initial field ψ_o^ε has a correlation radius of the order of ε^d (relative to the correlation radius of the index of refraction) for some $d\in(0,1)$, which means that it is larger than the wavelength (because $d < 1$) and smaller than the correlation radius of the index of refraction (because $d > 0$). The correlation function of the initial field is, therefore, of the form

$$\left\langle \psi_o^\varepsilon\left(x + \varepsilon^d\frac{y}{2}\right)\overline{\psi_o^\varepsilon}\left(x - \varepsilon^d\frac{y}{2}\right)\right\rangle = \mathcal{C}_o(y). \tag{11}$$

For the numerical simulations we consider the Gaussian model [62,63] in which $\mathcal{C}_o(y) = \exp[-y^2/(4\rho_o^2)]$. Finally, we consider the Wigner transform after a propagation distance of order ε^{-b} (relative to the correlation radius of the index of refraction):

$$W_z^\varepsilon(x,k) = \int_{\mathbb{R}} \left\langle \psi^\varepsilon_{\frac{z}{\varepsilon^b}}\left(x+\varepsilon^d\frac{y}{2}\right)\overline{\psi^\varepsilon_{\frac{z}{\varepsilon^b}}}\left(x-\varepsilon^d\frac{y}{2}\right)\right\rangle e^{-iky}dy. \tag{12}$$

In the scaling regime $d\in(1/5,1)$, $b = 1-d$, $c = 3(1-d)/2$, we get from Eq. (10) that it satisfies the scaled Vlasov-type equation

$$\partial_z W_z^\varepsilon + \partial_k\omega_k\partial_x W_z^\varepsilon - \frac{1}{\varepsilon^{b/2}}\partial_x V\left(\frac{z}{\varepsilon^b}, x\right)\partial_k W_z^\varepsilon = 0, \tag{13}$$

with the initial condition $W_{z=0}^\varepsilon(x,k) = \mathcal{W}_o(k) = \int_{\mathbb{R}} \mathcal{C}_o(y)e^{-iky}dy$ and with $\omega_k = \alpha k^2$ (see Ref. [57], sec. II). Note that the scaling of the potential in Eq. (13) is appropriate for the use of limit theorems for random differential equations ([64], Chapter 6) and we will carry out such a multiscale analysis.

Before going to the multiscale analysis, we remark that the solution of the Vlasov equation (13) can be expressed in terms of the solutions of random ordinary differential equations. Indeed, using the characteristic method, we have $W_z^\varepsilon(X_z^\varepsilon(x,k), K_z^\varepsilon(x,k)) = \mathcal{W}_o(k)$, where $(X_z^\varepsilon(x,k), K_z^\varepsilon(x,k))$ satisfies the ray equations

$$\frac{dX_z^\varepsilon}{dz} = 2\alpha K_z^\varepsilon, \quad \frac{dK_z^\varepsilon}{dz} = -\frac{1}{\varepsilon^{b/2}}\partial_x V\left(\frac{z}{\varepsilon^b}, X_z^\varepsilon\right), \tag{14}$$

starting from $X_{z=0}^\varepsilon(x,k) = x$, $K_{z=0}^\varepsilon(x,k) = k$. A key result (proved in Ref. [57], sec. III) that makes it possible to study the Wigner transform is the following one: For any $X, K\in\mathbb{R}$,

$$W_z^\varepsilon(X,K) = \int_{\mathbb{R}^2} \mathcal{W}_o(k)\delta[X_z^\varepsilon(x,k) - X]\delta[K_z^\varepsilon(x,k) - K]dxdk. \tag{15}$$

By taking an expectation (with respect to the distribution of the random medium), one can see that the mean Wigner transform involves the probability density function (PDF) of $(X_z^\varepsilon(x,k), K_z^\varepsilon(x,k))$. Higher-order moments of the Wigner transform involve multivariate PDFs. Those PDFs are computed in Ref. [57], sec. IV, and they give the following results.

Mean Wigner transform—From Eq. (15) we get the expression of the mean Wigner transform in the regime $\varepsilon \to 0$, which in turn gives the expression of the field correlation function $\mathbb{E}[\psi_z(x + (y/2))\overline{\psi_z}(x - (y/2))] = \mathcal{C}_o(y)\exp(-\gamma_2 z y^2/2)$, where $\gamma_2 = -\partial_x^2\gamma(0)$. This shows that the mean intensity is constant in z and x and that the correlation radius of the beam decays as $1/\sqrt{z}$ just as in the case of an initial coherent plane wave.

Scintillation index—We write the correlation function of the initial field in the dimensionless form $\mathcal{C}_o(y) = \tilde{\mathcal{C}}_o(y/\rho_o)$, where ρ_o is the correlation radius of the initial field. We introduce the relevant dimensionless parameter $X_o = \sigma^{2/3}\rho_o/\alpha^{1/3}$. We get that in the situation (pc) and (c) the scintillation index does not depend on x (see [57], sec. V):

$$S_z^{(\mathrm{pc})} = \tilde{\Pi}_{z/z_c}(0,0) - 1, \quad S_z^{(\mathrm{c})} = 2\tilde{\Pi}_{z/z_c}(0,0) - 1, \tag{16}$$

where $\tilde{\Pi}_{\tilde{z}}(\tilde{x},\tilde{y})$ is the solution to

$$\partial_{\tilde{z}}\tilde{\Pi}_{\tilde{z}} = i\partial_{\tilde{x}}\partial_{\tilde{y}}\tilde{\Pi}_{\tilde{z}} - \frac{1}{2}\left(\tilde{\Gamma}(0) - \tilde{\Gamma}(\tilde{x})\right)\tilde{y}^2\tilde{\Pi}_{\tilde{z}}, \tag{17}$$

starting from $\tilde{\Pi}_{\tilde{z}=0}(\tilde{x},\tilde{y}) = \tilde{\pi}_o(\tilde{y}/X_o)$. Here $\tilde{\Gamma}(\tilde{x}) = -\partial_{\tilde{x}}^2\tilde{\gamma}(\tilde{x})$, $\tilde{\pi}_o(\tilde{y}) = |\tilde{\mathcal{C}}_o(\tilde{y})|^2/\tilde{\mathcal{C}}_o(0)^2$, while Eq. (17) can be solved by a split-step Fourier method [53]. By expanding the solution of Eq. (17) for small $\tilde{z}$, we get $S_z^{(\mathrm{pc})} \simeq [\partial_{\tilde{x}}^4\tilde{\gamma}(0)/6](z/z_c)^3$, and $S_z^{(\mathrm{c})} \simeq 1 + [\partial_{\tilde{x}}^4\tilde{\gamma}(0)/3](z/z_c)^3$ at leading order, see Ref. [57], sec. VI [with $\partial_{\tilde{x}}^4\tilde{\gamma}(0) = 12\sqrt{\pi}$ for a medium with Gaussian correlation]. This shows that the early dynamics of the scintillation index in situation (pc) does not depend on the correlation radius ρ_o nor on the correlation function of the initial field, and is equivalent to the behavior valid for an initial plane wave. The scintillation index first grows cubically and then reaches

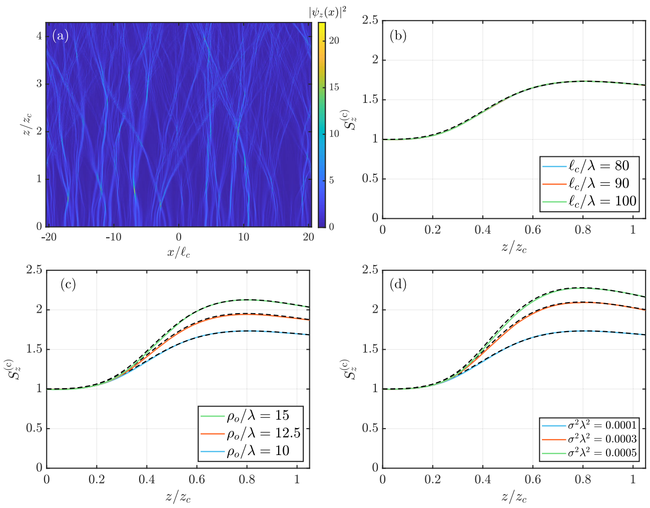

FIG. 3. Incoherent initial wave with a medium with Gaussian correlation. (a) Numerical simulation of Eq. (1) showing the evolution of $|\psi_z(x)|^2$ starting from a coherent speckle field [situation (c)], with $\rho_o/\lambda = 10$, $\ell_c/\lambda = 100$, $\sigma^2\lambda^2 = 10^{-4}$. (b)–(d) Evolution of $S_z^{(c)}$ versus z/z_c, by varying different parameters: the black dashed lines report the theory, Eq. (16); the colored lines are the results of the numerical simulations, averaged over 1000 independent realizations of the disordered potential and of the initial random field. Parameters: (b) $\rho_o/\lambda = 10$, $\sigma^2\lambda^2 = 10^{-4}$; (c) $\ell_c/\lambda = 100$, $\sigma^2\lambda^2 = 10^{-4}$; (d) $\rho_o/\lambda = 10$, $\ell_c/\lambda = 100$.

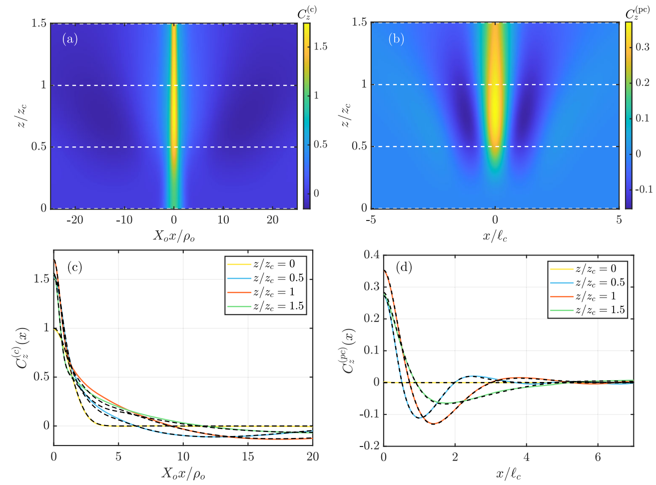

FIG. 4. Incoherent initial wave with a medium with Gaussian correlation. Theoretical intensity correlation function $C_z^{\mathcal{I}}(x)$: from Eq. (18) for a coherent speckle field (a) [situation (c)], and from Eq. (19) for a partially coherent speckle field (b) [situation (pc)]. (c)–(d) Corresponding comparison of the theoretical correlation function $C_z^{\mathcal{I}}(x)$ (black dashed lines), with the numerical simulations of Eq. (1) (colored lines), for different propagation lengths z/z_c. In situation (c), an average over 1000 realizations of $V(z,x)$ and of $\psi_o(x)$, has been considered. In situation (pc) an average over 300 realizations of $V(z,x)$, each with 400 realizations of $\psi_o(x)$. Parameters: $\ell_c/\lambda = 100$, $\rho_o/\lambda = 10$, $\sigma^2\lambda^2 = 10^{-4}$.

a maximum value, which depends on $X_o = \sigma^{2/3}\rho_o/\alpha^{1/3}$ only (it increases with X_o). It is interesting to note that X_o (and hence the maximal scintillation indices) depends on ρ_o but not on ℓ_c, while the distance z at which the maximum of the scintillation index is reached depends on ℓ_c through $z_c = \ell_c/(2\sigma^{2/3}\alpha^{2/3})$. Remember that when the initial field is a plane wave, the maximum of the scintillation index depends only on $X_c = \sigma^{2/3}\ell_c/\alpha^{1/3}$. This shows that speckled beams experience reduced intensity growth compared to plane waves: the smaller the correlation radius of the initial beam, the lower the maximal intensity reached by the beam as it propagates.

The theory (obtained in the limit $\varepsilon \to 0$) is compared to simulations of Eq. (1). The intensity evolution in Fig. 3(a) exhibits distinct qualitative features with respect to the coherent excitation in Fig. 1(a). As observed experimentally [42], in the coherent case, each branch is accompanied by sidelobes arising from interference effects, which tend to disappear when the initial condition is incoherent. In the simulations we study the impact of ρ_o, σ^2 and ℓ_c, on the scintillation index. Figure 3 shows an excellent quantitative agreement, in spite of the rather limited separation of scales of the parameters. The simulations also confirm that the maximum of S_z does not depend on ℓ_c, see Fig. 3(b).

Intensity correlation function—Our theoretical approach can be exploited to compute an explicit form for the fourth-order moments of the field. In particular, the intensity correlation function in situation (c) is

$$C_z^{\mathcal{I},(c)}(x) = \tilde{\Pi}_{z/z_c}(x/\ell_c, 0) + \tilde{\Pi}_{z/z_c}(x/\ell_c, X_o x/\rho_o) - 1. \quad (18)$$

This expresses a two-scale behavior: At the small scale $x \sim \rho_o$, the intensity correlation function decays rapidly, while its behavior exhibits complex variations at the large scale $x \sim \ell_c$. Similarly, the intensity correlation function in situation (pc) is given by

$$C_z^{\mathcal{I},(pc)}(x) = \tilde{\Pi}_{z/z_c}(x/\ell_c, 0) - 1. \quad (19)$$

Note that it is equal to $C_z^{\mathcal{I},(c)}(x)$ when x is of the order of ℓ_c because $\ell_c \gg \rho_o$ and $\tilde{\Pi}_{\tilde{z}}(\tilde{x}, \tilde{y}) \to 0$ as $\tilde{y} \to +\infty$. The intensity correlation functions are plotted in Fig. 4. The two-scale behavior of the intensity correlation function in situation (c) is clearly visible: the limit for large x/ρ_o of the intensity correlation function is the initial value for $C_z^{\mathcal{I},(pc)}$ (or $C_z^{\mathcal{I},(c)}$) when x is of the order of ℓ_c. This behavior can be seen in the numerical simulations as well in Fig. 4, and it satisfies the energy conservation relation $\int C_z^{\mathcal{I},(pc)}(x)dx = 0$.

Perspectives—We have reported a general stochastic theory of BFs by considering both coherent and incoherent initial waves. Optics naturally provides an ideal framework for experimentally testing and observing the theoretical predictions. The results presented in the two-dimensional framework can be extended to the three-dimensional one (see Ref. [57], sec. VII). Our work paves the way for a systematic approach to studying coherent phase-sensitive effects in BFs, focusing on the linear propagation regime. As shown in prior studies, linear BFs can trigger extreme nonlinear events [9–13,65–67], with intensity peaks significantly influenced by nonlinearity [9,68]. Our stochastic framework offers a basis for developing a theoretical model of nonlinear branched flow.

Acknowledgments—Funding was provided by Agence Nationale de la Recherche (Grants No. ANR-23-CE30-0021, No. ANR-21-ESRE-0040) and by Agence de l'Innovation de Défense (AID) via Centre Interdisciplinaire d'Études pour la Défense et la Sécurité (project PRODIPO). Calculations were performed using HPC resources from DNUM-CCUB (Université de Bourgogne Europe). A. P. acknowledges A. Tonello for valuable discussions during the initial phase of this work.

Data availability—No data were created or analyzed in this study.

[1] M. A. Topinka, B. J. LeRoy, R. M. Westervelt, S. E. J. Shaw, R. Fleischmann, E. J. Heller, K. D. Maranowski, and A. C. Gossard, Coherent branched flow in a two-dimensional electron gas, Nature (London) **410**, 183 (2001).
[2] K. E. Aidala, R. E. Parrott, T. Kramer, E. J. Heller, R. M. Westervelt, M. P. Hanson, and A. C. Gossard, Imaging magnetic focusing of coherent electron waves, Nat. Phys. **3**, 464 (2007).
[3] M. P. Jura, M. A. Topinka, L. Urban, A. Yazdani, H. Shtrikman, L. N. Pfeiffer, K. W. West, and D. Goldhaber-Gordon, Unexpected features of branched flow through high-mobility two-dimensional electron gases, Nat. Phys. **3**, 841 (2007).
[4] D. Maryenko, F. Ospald, K. v. Klitzing, J. H. Smet, J. J. Metzger, R. Fleischmann, T. Geisel, and V. Umansky, How branching can change the conductance of ballistic semiconductor devices, Phys. Rev. B **85**, 195329 (2012).
[5] B. Liu and E. J. Heller, Stability of branched flow from a quantum point contact, Phys. Rev. Lett. **111**, 236804 (2013).
[6] R. Höhmann, U. Kuhl, H.-J. Stöckmann, L. Kaplan, and E. J. Heller, Freak waves in the linear regime: A microwave study, Phys. Rev. Lett. **104**, 093901 (2010).
[7] S. Barkhofen, J. J. Metzger, R. Fleischmann, U. Kuhl, and H.-J. Stöckmann, Experimental observation of a fundamental length scale of waves in random media, Phys. Rev. Lett. **111**, 183902 (2013).
[8] E. J. Heller, R. Fleischmann, and T. Kramer, Branched flow, Phys. Today **74**, No. 12, 44 (2021).
[9] G. Green and R. Fleischmann, Branched flow and caustics in nonlinear waves, New J. Phys. **21**, 083020 (2019).
[10] Z.-Y. Sun and X. Yu, Nonlinear Schrödinger waves in a disordered potential: Branched flow, spectrum diffusion, and rogue waves, Chaos **32**, 023108 (2022).
[11] K. Jiang, T. W. Huang, R. Li, M. Y. Yu, H. B. Zhuo, S. Z. Wu, C. T. Zhou, and S. C. Ruan, Branching of high-current relativistic electron beam in porous materials, Phys. Rev. Lett. **130**, 185001 (2023).
[12] M. Mattheakis and G. P. Tsironis, Quodons in Mica, in *Extreme Waves and Branched Flows in Optical Media* (Springer International Publishing, New York, 2015), pp. 425–454.
[13] M. Mattheakis, I. J. Pitsios, G. P. Tsironis, and S. Tzortzakis, Extreme events in complex linear and nonlinear photonic media, Chaos Solitons Fractals **84**, 73 (2016).
[14] B. S. White and B. Fornberg, On the chance of freak waves at sea, J. Fluid Mech. **355**, 113 (1998).
[15] M. V. Berry, Tsunami asymptotics, New J. Phys. **7**, 129 (2005).
[16] M. V. Berry, Focused tsunami waves, Proc. R. Soc. A **463**, 3055 (2007).
[17] E. J. Heller, L. Kaplan, and A. Dahlen, Refraction of a Gaussian seaway, J. Geophys. Res. **113**, C09023 (2008).
[18] L. H. Ying, Z. Zhuang, E. J. Heller, and L. Kaplan, Linear and nonlinear rogue wave statistics in the presence of random currents, Nonlinearity **24**, R67 (2011).
[19] H. Degueldre, J. J. Metzger, T. Geisel, and R. Fleischmann, Random focusing of tsunami waves, Nat. Phys. **12**, 259 (2016).
[20] M. A. Wolfson and S. Tomsovic, On the stability of long-range sound propagation through a structured ocean, J. Acoust. Soc. Am. **109**, 2693 (2001).
[21] M. Mattheakis, G. P. Tsironis, and E. Kaxiras, Emergence and dynamical properties of stochastic branching in the electronic flows of disordered Dirac solids, Europhys. Lett. **122**, 27003 (2018).
[22] K. Jose, N. Ferguson, and A. Bhaskar, Branched flows of flexural waves in non-uniform elastic plates, Commun. Phys. **5**, 152 (2023).
[23] A. Brandstötter, A. Girschik, P. Ambichl, and S. Rotter, Shaping the branched flow of light through disordered media, Proc. Natl. Acad. Sci. U.S.A. **116**, 13260 (2019).
[24] J. St'avina and P. Bokes, Quantum and classical branching flow in space and time, Phys. Rev. A **106**, 052215 (2022).
[25] A. Daza, E. J. Heller, A. M. Graf, and E. Räsänen, Propagation of waves in high Brillouin zones: Chaotic branched flow and stable superwires, Proc. Natl. Acad. Sci. U.S.A. **118**, e2110285118 (2021).
[26] A. Wagemakers, A. Hartikainen, A. Daza, E. Räsänen, and M. A. F. Sanjuán, Chaotic dynamics creates and destroys branched flow, Phys. Rev. E **111**, 014214 (2025).
[27] K. H. Mok and R. Fleischmann, Branched flows in active random walks and the formation of ant trail patterns, Phys. Rev. Res. **5**, 043299 (2023).
[28] A. Patsyk, U. Sivan, M. Segev, and M. A. Bandres, Observation of branched flow of light, Nature (London) **583**, 60 (2020).
[29] S. Chang, K.-H. Wu, S. Liu, Z.-K. Lin, J. Wu, S. Ge, L.-J. Chen, P. Chen, W. Hu, Y. Xu, H. Chen, D. He, D.-Q. Yang, J.-H. Jiang, Y. Lu, and J. Chen, Electrical tuning of branched flow of light, Nat. Commun. **15**, 197 (2024).
[30] S. Rotter and S. Gigan, Light fields in complex media: Mesoscopic scattering meets wave control, Rev. Mod. Phys. **89**, 015005 (2017).

[31] H. Cao, A. P. Mosk, and S. Rotter, Shaping the propagation of light in complex media, Nat. Phys. **18**, 994 (2022).

[32] V. Kulkarny and B. S. White, Focusing of waves in turbulent inhomogeneous media, Phys. Fluids **25**, 1770 (1982).

[33] D. I. Zwillinger and B. S. White, Propagation of initially plane waves in the region of random caustics, Wave Motion **7**, 207 (1985).

[34] M. V. Berry and C. Upstill, IV catastrophe optics: Morphologies of caustics and their diffraction patterns, Prog. Opt. **18**, 257 (1980).

[35] J. F. Nye, *Natural Focusing and Fine Structure of Light: Caustics and Wave Dislocations* (CRC Press, Boca Raton, 1999).

[36] L. Kaplan, Statistics of branched flow in a weak correlated random potential, Phys. Rev. Lett. **89**, 184103 (2002).

[37] J. J. Metzger, R. Fleischmann, and T. Geisel, Universal statistics of branched flows, Phys. Rev. Lett. **105**, 020601 (2010).

[38] J. J. Metzger, R. Fleischmann, and T. Geisel, Statistics of extreme waves in random media, Phys. Rev. Lett. **112**, 203903 (2014).

[39] M. Pradas, A. Pumir, and M. Wilkinson, Uniformity transition for ray intensities in random media, J. Phys. A **51**, 155002 (2018).

[40] J. J. Metzger, R. Fleischmann, and T. Geisel, Intensity fluctuations of waves in random media: What is the semiclassical limit?, Phys. Rev. Lett. **111**, 013901 (2013).

[41] M. V. Berry, Elementary branching: Waves, rays, and decoherence, J. Opt. **22**, 115608 (2020).

[42] A. Patsyk, Y. Sharabi, U. Sivan, and M. Segev, Incoherent branched flow of light, Phys. Rev. X **12**, 021007 (2022).

[43] L. C. Andrews and R. L. Phillips, *Laser Beam Propagation through Random Media* (SPIE-International Society for Optical Engineering, Bellingham, 2005).

[44] V. I. Tatarskii, *Waves Propagation in a Turbulent Medium* (McGraw-Hill, New York, 1961).

[45] B. Crosignani, B. Daino, and P. Di Porto, Light scattering by a rotating disk, J. Appl. Phys. **42**, 399 (1971).

[46] J. W. Goodman, *Speckle Phenomena in Optics: Theory and Applications*, 2nd ed. (SPIE Press, Bellingham, 2020).

[47] B. I. Erkmen and J. H. Shapiro, Unified theory of ghost imaging with Gaussian-state light, Phys. Rev. A **77**, 043809 (2008).

[48] J. H. Shapiro and R. W. Boyd, The physics of ghost imaging, Quantum Inf. Process. **11**, 949 (2012).

[49] A. Ishimaru, *Wave Propagation and Scattering in Random Media* (Academic Press, New York, 1978).

[50] J. Garnier and K. Sølna, Scintillation in the white-noise paraxial regime, Commun. Partial Differ. Equations **39**, 626 (2014).

[51] J. Garnier and K. Sølna, Fourth-order moments analysis for partially coherent electromagnetic beams in random media, Waves Random Complex Media **33**, 1346 (2023).

[52] This results from the fact that, for z large, the correlation function has the form $\exp(-\gamma_2 z y^2/2)$, where $\gamma_2 = -\partial_x^2\gamma(0) = \sigma^2\ell_c^{-1}\tilde{\gamma}_2$, $\tilde{\gamma}_2 = -\partial_{\tilde{x}}^2\tilde{\gamma}(0)$, is always positive because it is proportional to the power spectral density of the stationary process $\partial_x V(z,0)$ at frequency 0.

[53] G. Strang, On the construction and comparison of difference schemes, SIAM J. Numer. Anal. **5**, 506 (1968).

[54] J. Garnier and K. Sølna, Fourth-moment analysis for beam propagation in the white-noise paraxial regime, Arch. Ration. Mech. Anal. **220**, 37 (2016).

[55] G. Bal and A. Nair, Complex Gaussianity of long-distance random wave processes, arXiv:2402.17107.

[56] G. Bal and A. Nair, Long distance propagation of light in random media with partially coherent sources, arXiv:2406.05252.

[57] See Supplemental Material at http://link.aps.org/supplemental/10.1103/PhysRevLett.134.223803 for the theoretical developments and details about the numerical simulations, which includes Refs. [58–61].

[58] J. L. Synge, The Hamiltonian method and its application to water waves, Proc. R. Irish Acad., Sect. A **63**, 1 (1963).

[59] J. Garnier and K. Sølna, Coupled paraxial wave equations in random media in the white-noise regime, Ann. Appl. Probab. **19**, 318 (2009).

[60] J. Garnier and K. Sølna, Scaling limits for wave pulse transmission and reflection operators, Wave Motion **46**, 122 (2009).

[61] L. Isserlis, On a formula for the product moment coefficient of any order of a normal frequency distribution in any number of variables, Biometrika **12**, 134 (1918).

[62] J. T. Foley and M. S. Zubairy, The directionality of Gaussian Schell-model beams, Opt. Commun. **26**, 297 (1978).

[63] A. T. Friberg and R. J. Sudol, Propagation parameters of Gaussian Schell-model beams, Opt. Commun. **41**, 383 (1982).

[64] J.-P. Fouque, J. Garnier, G. Papanicolaou, and K. Sølna, *Wave Propagation and Time Reversal in Randomly Layered Media* (Springer, New York, 2007).

[65] J. M. Dudley, F. Dias, M. Erkintalo, and G. Genty, Instabilities, breathers and rogue waves in optics, Nat. Photonics **8**, 755 (2014).

[66] A. Safari, R. Fickler, M. J. Padgett, and R. W. Boyd, Generation of caustics and rogue waves from nonlinear instability, Phys. Rev. Lett. **119**, 203901 (2017).

[67] J. M. Dudley, G. Genty, A. Mussot, A. Chabchoub, and F. Dias, Rogue waves and analogies in optics and oceanography, Nat. Rev. Phys. **1**, 675 (2019).

[68] K. Jiang, T. W. Huang, C. N. Wu, M. Y. Yu, H. Zhang, S. Z. Wu, H. B. Zhuo, A. Pukhov, C. T. Zhou, and S. C. Ruan, Nonlinear branched flow of intense laser light in randomly uneven media, Matter Radiat. Extremes **8**, 024402 (2023).